

Detour-Impact Index Method and Traffic Gathering Algorithm for Assessing Alternative Paths of Disrupted Roads

Alessandro Pucci

Department of Civil Engineering
University of Minho, ISISE, Department of Civil Engineering, Guimarães, Portugal, 4800-058
Email: ale@civil.uminho.pt
ORCID: <https://orcid.org/0000-0001-6733-8864>

Mario Lucio Puppio

Department of Energy, Systems, Territory and Constructions Engineering
University of Pisa. Pisa, Italy, 56122
Email: m.puppio@ing.unipi.it
ORCID: <https://orcid.org/0000-0003-1474-7853>

Hélder Silva Sousa

Department of Civil Engineering
University of Minho, ISISE, Department of Civil Engineering, Guimarães, Portugal, 4800-058
Email: hssousa@civil.uminho.pt
ORCID: <https://orcid.org/0000-0002-4569-1090>

Linda Giresini

Department of Energy, Systems, Territory and Constructions Engineering
University of Pisa. Pisa, Italy, 56122
Email: linda.giresini@unipi.it
ORCID: <https://orcid.org/0000-0001-6913-7468>

José Campos Matos

Department of Civil Engineering
University of Minho, ISISE, Department of Civil Engineering, Guimarães, Portugal, 4800-058
Email: jmatos@civil.uminho.pt
ORCID: <https://orcid.org/0000-0002-1536-2149>

Mauro Sassu

Department of Civil, Environmental Engineering and Architecture
University of Cagliari. Cagliari, Italy, 09123
Email: msassu@unica.it
ORCID: <https://orcid.org/0000-0002-3414-2360>

Accepted Version

ABSTRACT

Infrastructures play a key role in society. Recent collapses of bridges have underlined their importance for the road functionality, causing disruptions to commuters and emergency vehicles. Major issues arise on rural roads, where the lack of redundancy led to the isolation of entire communities. Actual approaches to assess the resilience of countryside streets rely on the availability of specific datasets, limiting the practical applications; this issue is typically related to traffic data. This research aims to propose innovative algorithms to assess the road network's vulnerability in rural areas, including a novel traffic data collection process and its calibration. The aggregate metric is called Detour-Impact Index (DII) and compares the users' costs before and after a disruptive event. The method uses traditional network-impact metrics in combination with a new algorithm that allows to gather quantitative traffic data starting from qualitative information. Users' travel time showed good agreement between the proposed procedure and traditional web-based methods. Furthermore, the paper provides users' delay costs functions accounting for traffic composition, trips' purposes, vehicles' operative costs, nonlinear volume-capacity relation, and average daily traffic. A significant aspect is the adaptability of this framework, as it is designed to be coupled with existing approaches. The method is demonstrated on a case study in Tuscany (Italy).

Keywords: Transportation Network, Traffic Engineering, Risk Management, Bridge Failure, Transportation Management

INTRODUCTION

Civil infrastructures play a vital function in the management of crisis and commuters' daily trips (1). The vulnerability to bridges from hazardous events has been extensively investigated (2). Both businesses and rescue activities are affected by infrastructures' collapses. One important issue concerns the connection between strategic buildings (i.e. hospitals, collective shelters) and countryside' settlements (3). In those areas, a road link failure might cause the isolation of entire communities. The problem arises mostly due two aspects: (i) the maintenance of secondary infrastructures and (i) the lack of network redundancy (4). This introduces the problem of quantifying the vulnerability of secondary infrastructures. Several authors over the last two decades looked at disruptions on roads, usually by defining a performance indicator. Reviews of such metrics are given in (5), (6). The body of work revealed that one metric above all has been widely applied: the Network Robustness Index (NRI) developed by Scott et al. (7). The study was the first to demonstrate the importance of network connectivity beside the traditional volume-capacity ratio. In his pioneering work, Scott et al. (7) associated the travel-time cost to the link performance. This was the key to prove how a local disruption has a system-wide impact. The concept was taken over by Nagurney and Qiang (8). The network efficiency introduced the ratio between travel demand and the minimum time associated to an origin-destination pair. Furthermore, the drop of efficiency is assessed comparing the pre- and post-disruption conditions. Nevertheless, both metrics cannot account for trips' purposes. Sullivan et al. (9) tried to overcome this limitation proposing a modified NRI, known as Network Trip Robustness (NTR). A further approach, that combines local and global metrics has been proposed by Rupi et al. (10). The links are ranked based on a local and a global importance index. The former refers to the Average Daily Traffic (ADT), while the latter to the variation in trips' costs. The authors drew the attention on the possibility of having a poor dataset and its implications on the analysis' outcome. Although researchers proposed different methods, the impact of a closed link on the network is always assessed based on the difference in performance before and in the aftermath of a disruption. The main variation relies upon the alternative metrics adopted. The generalised travel cost is one of the most used (11). A different approach highlighted the missed cascade effect on traditional path-based scenarios (12). The single link closure might hide the combined losses of multiple link disruption at a time. To account for multi-roads failure, several authors have recently tried to link the hazard simulation (e.g. floods, earthquakes) with network disruption scenarios (13). An example of such integrated approaches can be found in Arrighi et al. (14). The main difference to classical transportation approaches is the direct dependence of the accessibility index on the hazard return period. Despite the existence of such advanced methods, there is still the research need to propose new algorithms to account for datasets availability in rural areas. Typically, road network analysis problems can be implemented if traffic data is known. For densely populated areas, there is often the availability of traffic information collected by cameras and traffic sensors, whereas the countryside' scenario is quite different (15). The budget constraint is a decisive factor to local authorities in collecting the traffic data (16), leaving the statistical analysis the most used in practice, despite its limitations (17). More recently, the use of web-based traffic data was found to be a valid alternative to the abovementioned methods. Since the release of Google maps API, it was possible to gather traffic data without the disadvantages of the statistical models (18). Most of these tools rely on the public version of the API, which represents one of its advantages as it is an open access resource (19). The image processing technique applied to Google maps is of particular interest (20), as a specific algorithm was designed to extract the value of congestion of several streets using a histogram of colours. In the present study, the idea is repeated with the major purpose of combining the image analysis with engineering theory to quantitatively estimate the traffic on roads. This work presents a parallel approach compared to the newest ones, that usually rely on the use of crowdsourced data (21). In here, the methodology is focused on the use of a web image-based algorithm to gather qualitative data and using traffic engineering theory to transform it into quantitative information. Furthermore, this work directly answers to the research need of specifically addressing the combination of the following issues: (i) account for trips' purposes; (ii) estimate the percentage of heavy vehicles on traffic flow; (iii) estimate the vehicles' operative costs related to cars and trucks; (iv) explicitly account for the speed reduction based on the nonlinear volume-capacity ratio. Although some of these parameters have been investigated, as the willingness to pay for each extra-minute of driving (22), there is still the need to merge different approaches and disciplines to assess the disruption on rural roads. Whereas there are more complex approaches that account both for traffic and hazard simulation methods (23), the present

study is focused to demonstrate a possible strategy to the mentioned research needs. The method has been conceived in modules: each step can be further improved or adjusted, including for example a disruption management module (23) as well as a human-made or natural hazard simulation module (24). The paper shows how to practically assess the performance of a road network by comparing users' costs in the aftermath of a disruptive event versus stationary pre-event conditions. The framework is also focused on data availability issues, by developing an innovative quantitative traffic gathering method from qualitative information. The applicability of the method is tested on a real network located in Tuscany (Italy). The paper is organized in four main sections. This section introduces the problem examining past literature regarding road network performance indicators and traffic data availability. In Methods the proposed framework is described, whereas in Application a case study is presented. The resulting implications are discussed in the Conclusions.

METHOD

The most vulnerable component of the infrastructure system is represented by bridges (25). This has been demonstrated in case of inundations, in which the bridge collapse caused a longer downtime compared to temporary flooded road links (26). In addition to this challenge, in rural areas traffic data is often unavailable, leaving the bridge manager to deal with both local and network issues. Hence, the proposed framework is focused on providing a tool with a wide applicability, especially for those areas in which data availability represents a serious issue. The output of the model consists in a performance indicator called Detour-Impact Index (DII). It is defined in **Equation 1** as the ratio of the increased users' costs in the aftermath of a disruption to the pre-event condition. It is distinguished from existing metrics as it explicitly accounts for cost-specific functions rather than generalised ones. Thus, the DII considers the sum of a delay-cost function (DC) and a vehicle's operational cost (VOC). These depend on: (i) traffic average speed based on a non-linear volume-capacity relation; (ii) Average Daily Traffic (ADT) along each link; (iii) driver's time cost function (DTC) and (iv) traffic composition (i.e. percentage of trucks), see **Equations 3, 4**. The DII is also explained through the graphical support of Error! Reference source not found..

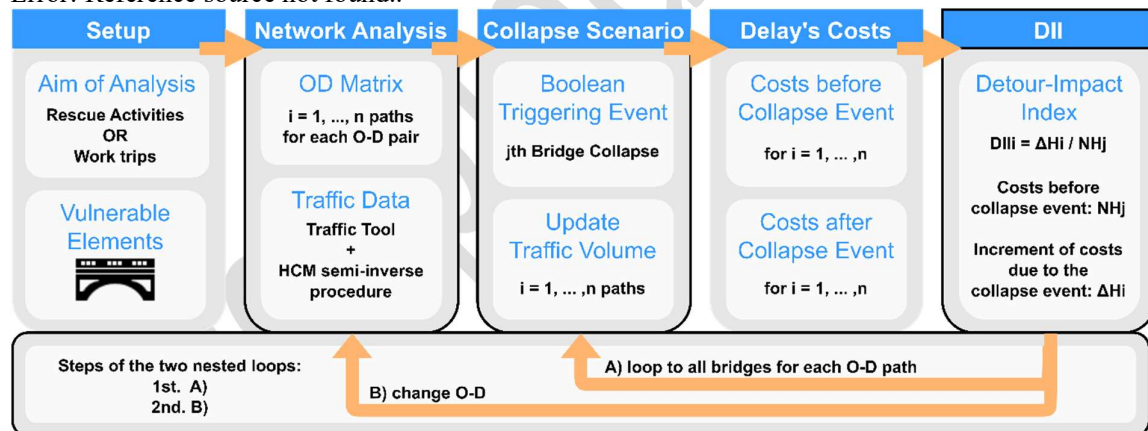


Figure 1. Flowchart of the Detour – Impact Index Method

$$DII_i = \Delta H_i / NH_j \quad (1)$$

Being $i = 1, \dots, n$ the alternative paths; j the path closed due to the failure of a network component; ΔH is the increment of costs (in €) related to the post-hazard scenario; NH the costs (in €) assessed in the no-hazard scenario. The greater is DII, the higher is the impact of the traffic-related costs. It should be highlighted that in Equation 1 the increased cost on alternative paths is normalised to that of closed route, during normal operations. This allows for the estimation of the impact of the detour, useful for regular users in case of closed path. Three types of expenditures must be appraised for each i -th alternative: (i) The normal-operational costs in the j -th path and (ii) in the i -th one; (iii) The post-hazard costs in the i -th path. Hence, the parameter ΔH can be evaluated for each link by subtracting the costs obtained in the post-hazard scenario ($DC_k + VOC_k$) on the i -th path, to the ones in

the normal condition ($NC_k + NVOC_k$) as in **Equation 2**; where, $k = 1, \dots, m$ are the links of the selected i -th path connecting the O-D for the selected i -th path, as in Error! Reference source not found..

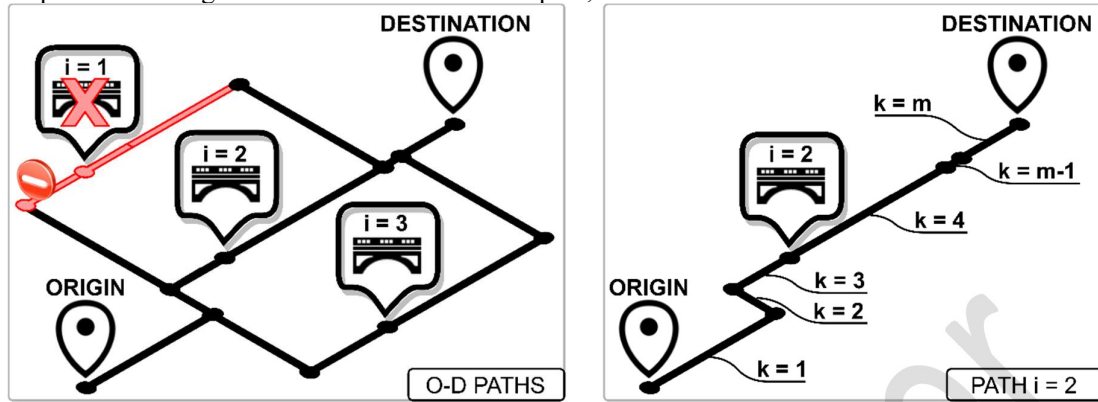


Figure 2. Failures and alternative paths. Overall network for OD pairs (left) in which $i=1$ is taken as the j -th path. Links for costs computation on the alternative path $i = 2$ (right)

$$\Delta H_i = \sum_{k=1}^m (DC_{ik} + VOC_{ik}) - (NC_{ik} + NVOC_{ik}) \quad (2)$$

It is not possible to compute ΔH looking only at the post-hazard scenario, since in that case the information presented by the previous **Equation 2** without the ($NC_k + NVOC_k$) term, would have provided the total expenditures including the component of traffic during the normal-operational conditions; this concept is clearer looking at the daily delays' costs, DC_k as in **Equation 3**.

$$DC_{ik} = T_{aik} \cdot 1day \cdot ADT_{ik} \cdot \sum_{r=1}^4 (DTC_{ir} \cdot p_{ir}) \quad (3)$$

Being $T_{aik} = L_{ik}/S_{aik}$ the k -th link traversal time; S_{aik} is the reduced speed obtained through the updated volume-capacity ratio of the street; L_{ik} is the k -th link length; ADT_{ik} is the average daily traffic on the k -th link of the i -th alternative path. The traffic assignment problem is based on a system optimal management, even though other assignments can be performed, as shown in the section "Collapse Scenario". The DTC_{ir} is the cost per unit of time (hours) associated to the users' trip purpose, namely a person having a work or non-work trip and driving a r -class vehicle, according to Gervásio and Simões (27). The most common scenario in rural areas is represented by commuters' journeys (i.e. work trips), while for more refined analyses, the ADT_{ik} can be splitted between work and non-work trips based on census data and local surveys. In this more complex setup, the indirect costs' computation shall be performed separately and added before computing the DII. The percentage of vehicle's type in traffic composition is indicated with the symbol p_{ir} . The equivalent parameter NC_{jk} is evaluated accordingly, but including the ADT_j term and the normal operation speed S_{nik} . The vehicle's operational cost (VOC) is computed according to (27) changing the equation syntax for a better application to the proposed framework. Hence, the VOC_{ik} is evaluated as in **Equation 4**.

$$VOC_{ik} = -\frac{S_{pik}}{S_{nik}} \cdot L_{ik} \cdot 1day \cdot ADT_{ik} \cdot \sum_{r=1}^4 (DTC_{ir} \cdot p_{ir}) \quad (4)$$

In both parameters, namely VOC_{ik} and $NVOC_{ik}$, the present speed S_{pik} is introduced. In VOC_{ik} , $S_{pik} = S_{aik}$, while during normal conditions, $S_{pik} = S_{nik}$. This distinction is made jointly with a negative value VOC terms, because the vehicle's operative cost is maximum when $(L_{ik} - S_{pik}/S_{nik} \cdot L_{ik})$ attains the largest value, i.e. when $S_{pik} = S_{aik}$. Hence, $VOC_{ik} - NVOC_{ik}$ in **Equation 2** returns $(L_{ik} - S_{aik}/S_{nik} \cdot L_{ik})$ which is the difference between operative expenditures of vehicles at normal speed S_{nik} and reduced one, S_{aik} . The parameter $NVOC_j$ is assessed accordingly, with the same recommendation about the ADT_j term and without the minus sign, because no difference is appraised but only the operative costs due to the volume of traffic ADT_{jk} . The DII is just the output of the framework, while the whole methodology involves five steps: (i) delimitation of the area under study; (ii) acquisition of road network's and bridges' maps; (iii) identification of settlements and build an Origin Destination (O-D) matrix to

generate the paths; (vi) use of the developed Traffic tool algorithm to analyse congestion scenarios; (v) assumption of a collapse scenario for each infrastructure and assessment of DII. The flowchart of the methodology is illustrated in **Figure 2** and theoretically discussed in this Section whereas it is used in a case study in the Application Section.

Setting up of the GIS environment and preliminary analysis of the area under study

The selection of the area under study is made using a GIS tool. Administrative boundaries delimitate the portion of territory. As the framework is tailored on rural areas, other contexts were not investigated. Despite this assumption, the theoretical model of the framework is still valid also on urban areas. In cities only a higher computational effort is required, due to the increased density of bridges, roads and thus, alternative paths. This issue cannot be taken for granted, but on urban areas the availability of more data justifies the adoption of existing methods. Hence, the proposed framework demonstrates its usefulness in rural contexts. The second step consists in gathering the road network's map and the bridge location vector, within the area under study. This task can be performed by using GIS maps. The data-availability issue is highlighted as a possible missed dataset of bridges' location. Two procedures are proposed to overcome this problem. The road network map can be considered as a graph $G(S, N)$, made up by links (S) and nodes (N), being n_S the number of links and n_N the number of nodes. The bridges' location vector B has n_B elements. The following two procedures are applicable in case of missing B . Procedure 1: Consider S in which each link has an elevation attribute, that on Jedlička et al. (28) assumes the following values: $Z_i = \{-1, 0, 1\}$. A bridge $b \in R^{n_B}$ can be identified using the following expression: $B = Z_0 \cap Z_1$, given $Z_0 \subseteq S$ and $Z_1 \subseteq S$. The second method allows to find $b \in R^{n_B}$ on watercourses. Procedure 2: Given a river network map W made up of n_W segments, then $B = (W \cap Z_0) \cup (W \cap Z_1)$. The study also requires knowledge about the strategic buildings position. These data can be found in Emergency Limit Condition (ELC) maps (29). It is crucial to note that either bridges, strategic structures and infrastructure links, as a design purpose, can be reduced in number depending if a hazard simulation scenario is run in parallel to this analysis. Then, settlements are identified with the destination vector D , where $D \subset N$. In such way, the arrival point is part of the graph G , and routing algorithms as Dijkstra can be used (30). The next step concerns the origin-destination (O-D) matrix design. Each small town is linked to the Civil Protection headquarters, connecting one Origin to several Destinations. Each O-D pair P includes n_P paths, each $p \in R^{n_P}$ can be created using existing routing algorithms (31). Each path is made up by a set of links $k = 1 \dots m$ (**Figure 1**), each characterized by a traffic volume v_k . Theoretically one can assume that the volume of vehicles is known, but on practical applications, data availability on rural roads is an issue. Thus, an innovative web-based method has developed to gather traffic data, and is illustrated in the next section.

Traffic data acquisition

The new method, shown in **Figures 3-6**, starts looking at web-based traffic layers as the Google Maps' one. These layers are qualitative, but it is the Authors' conviction that they can be considered as an immediate, simple and effective tool to gather information on traffic conditions in absence of counters. Indeed, the proposed method is not intended to substitute the more reliable traditional in-situ counting techniques, but instead to give a first estimation of the traffic quality. The main idea behind the proposed procedure is to populate each v_k vector with a quantitative information gathered using a two-step method: (i) use of Traffic Tool script to gather qualitative data; (ii) use an algorithm to transform qualitative traffic information into volumes of vehicles.

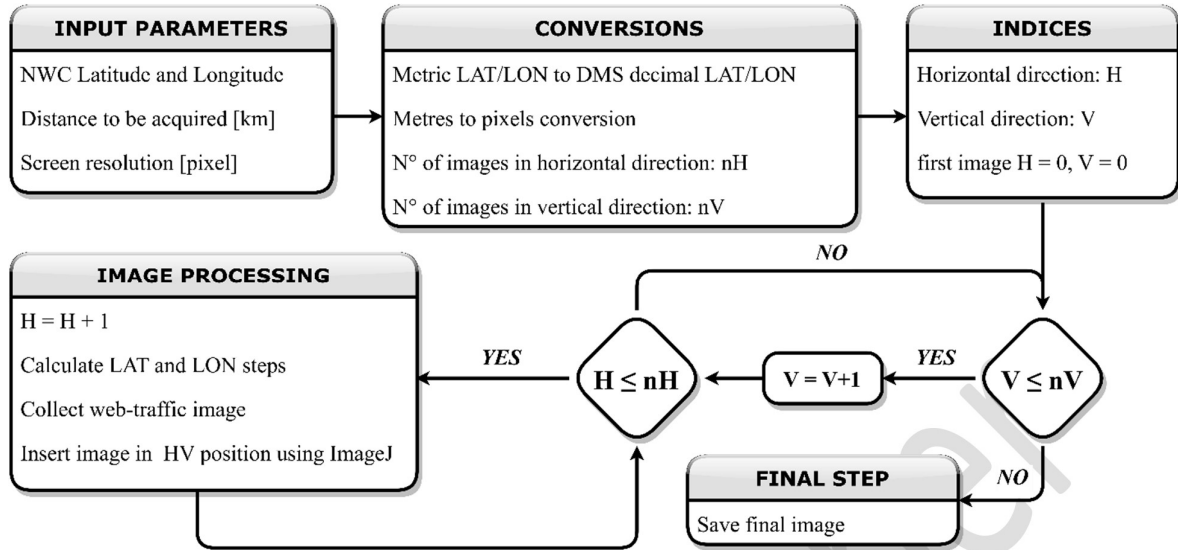


Figure 3. Traffic Tool script flowchart

Traffic script

Firstly, the qualitative data visualized in the web map traffic layer is collected using a script named Traffic Tool developed by the Authors. The script has been developed using ImageJ software (32). The algorithm’s flowchart is highlighted in **Figure 3** and its code can be found in the Appendix of this paper. The script captures single web-images as from Google Maps, at different latitude/longitude coordinates and appropriately merges them into a single (bigger) image. In this way the final picture looks like a single high-definition image. The merging phase is conducted using a matricial order, by performing two nested loops: one for latitude calculation (rows of the matrix) and the other for longitude (columns of the matrix). **Figure 4** shows a practical example of the assembly process. Then, one raster per each web-based traffic color is generated by means of another IJ1 script, provided together with the Traffic Tool. Each image is then overlaid with the road network shapefile on GIS. This can be done by importing the raster that comes with the tfw companion file, which is also created by the Traffic Tool. Hence, by employing GIS plugins, the properties of each raster can be included into the shapefile. An additional column is created on the attribute table of each $p \in R^n$. User supervision is always required along these automated steps, as sporadic manual adjustments might be necessary. The traffic colours from web-based maps as Google’s one, are labelled as follows: green = AB; orange = CD; red = E; dark red = F. The labels are used to populate the newly created column on each p vector file. The result is a road network shapefile with qualitative traffic information. As the simulations are performed by using web-based traffic, multiple simulations can be performed at local peak hours, or at specific time, depending on the aim of the analysis.

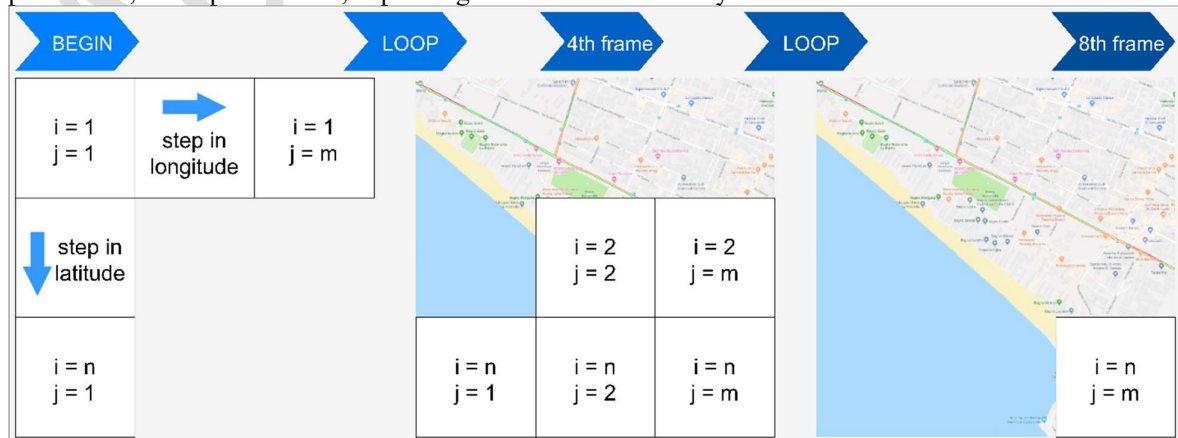


Figure 4. Assembly process – image from Google Maps©

From qualitative to quantitative traffic data

The qualitative information is transformed into quantitative one, using a new algorithm that incorporates equations included in the Highway Capacity Manual (HCM) (33). The process is described in **Figure 5**. The qualitative traffic obtained using Traffic Tool is compared to the Level Of Service (LOS) defined by the HCM. The criterion is established according to **Figure 6**. The motivations for such a choice can be explained from the definition of each qualitative metric. For example, Google stated that the traffic colours represent the delay due to various grades of congestion (34). On the other side, the LOS is a traffic performance indicator. Hence, the qualitative relationship between the two indices can be based on the expected-delay level. Since there are four levels in Google traffic and six in the LOS, a clustering of the HCM index is proposed. A further innovation relies on the use of LOS as input, while traditionally is an output. A reverse-phased method is then adopted. This allows for the computation of quantitative traffic volumes. Each LOS is associated to an interval of traffic speed. The mean value of each speed range S_{LOS} is assumed. Then, the link traversal time R_t can be calculated, with the simple relation $R_t=L/S_{LOS}$, where L is the link length. Similarly, the link traversal time at free-flow speed R_0 can be evaluated by using the HCM. Hence, the quantitative traffic volume, which is based on road links' LOS, can be found using the following **Equation 5**. More in detail, the volume of vehicles is derived from the images acquired using the script provided in the Appendix of this paper. This script is also included in GIS environment through the procedures described in the previous subsection.

$$v = \left\{ \frac{[T \cdot (R_t - R_0) + 2(R_t - R_0)^2]}{[2JL^2 + T(R_t - R_0)]} \right\} c \quad (5)$$

Where J is a calibration parameter whose values are specified in the HCM, c is the capacity of the street (vehicles/hour) obtained from OTM maps (28), T is the reference period (typically 1 hour). It should be noticed that the previous equation does not consider the delay due to signalized intersections. This can be an issue in an urban area with many traffic lights, but not in rural areas. The traffic volume obtained through **Equation 5** is related to the ADT term on **Equation 3, 4**, and thus is directly linked to the DII. To obtain the ADT, the volume in veh/h has to be divided by the hourly volume factor that can be assumed equal to 0.10. The traffic volume computation sets the stage for the next step which introduces the collapses.

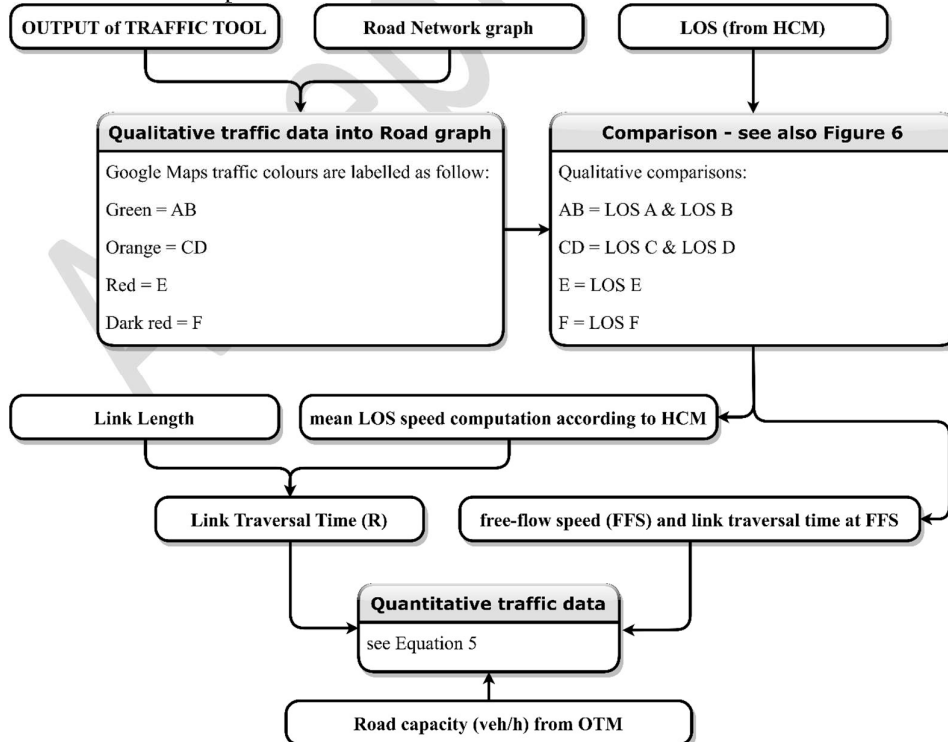


Figure 5. Quantitative traffic assessment flowchart

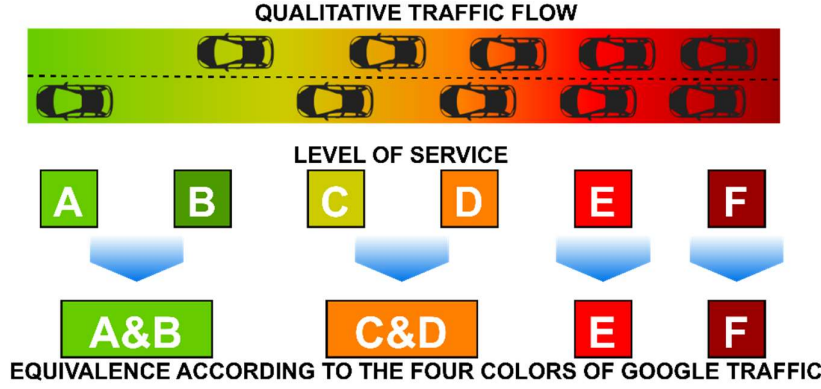


Figure 6. Example of LOS levels reduction to the corresponding web-based map classification (in this case Google Traffic)

Collapse scenario

All data collected and elaborated until this point is employed to simulate the consequences of a failure in a road. Firstly, the road network is converted to a routable graph. Briefly, in each crossing a node is generated according to the map's topology. Directions properties are introduced in the network and edges act as connectors between nodes. Then, all the paths between an O-D couple are generated using a routing plugin. To this end, existing algorithms with a GIS interface can be employed (35). This aspect is crucial when alternative paths are considered. Each route contains information on traffic volumes calculated with **Equation 5**. Then, for each O-D path, the following **Equation 6** (adapted from HCM) is assumed to evaluate the traversal time R_c expressed in hours, during the collapse scenario.

$$R_c = R_0 + 0.25 \left[\frac{v_{upd}}{c} - 1 + \sqrt{\left(\frac{v_{upd}}{c} - 1\right)^2 + \frac{16J \cdot v_{upd}}{c} L^2} \right] \quad (6)$$

where v_{upd}/c is the volume-capacity ratio that received the detoured traffic from the collapsed link, as demonstrated below. The total travel time of a specified O-D path is the sum of all computed R_c values for each link of length L . To generate the failure scenario, all the paths for each O-D pair are considered. The DII computation is demonstrated according to the design in **Figure 7**, in which bridges' position is determined by the intersection between the links $a, b, c, \in S$ and the river $w \in W$. The failure of a bridge is taken as a Boolean event in this study, whereas the collapse probability can be appraised using existing hazard simulation models coupled with an appropriate structural analysis (36). The collapse scenario has the effect of detouring the traffic volume of one path to the alternative one using a system-optimal assignment. Nevertheless, the proposed method can also accommodate other traffic assignments such as the user equilibrium. To briefly demonstrate this capability and summarise the workflow, an example is presented on a simple 3-links network, according to **Figure 7**. Once that R has been calculated using **Equation 6**, the economic costs can be computed, to determine which alternative path is the most critical. The computation for the network in **Figure 7** is done according to the following workflow:

```

For p = 1 to  $n_p$  do # $n_p$  = number of paths (3 in the network of Figure 7)
   $V_{detour} = V_p$  #the volume to detour ( $V_{detour}$ ) is the traffic on the closed path ( $V_p$ )
  For iteration = 0 to  $V_b$  do
    For i = 1 to  $n_b$  do # $n_b$  = number of bridges (3 in the network of Figure 7)
      If i = p then
        i = i + 1
      else
        Traffic Assignment computation
        compute DII;

```

According to the example, the input parameters are shown in **Table 1**.

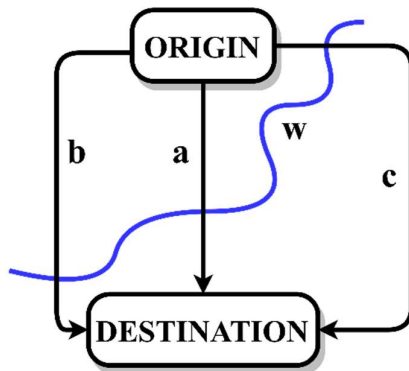


Figure 7. Network intersecting a river to highlight bridges' locations

TABLE 1. Example parameters and their source for the network of Figure 7.

Source:	Dijkstra on GIS	Traffic Tool	OTM	HCM	HCM	Equation 5
Route	Length	LOS	Capacity	Av. Speed	FFS	Volume
a	2 km	E	800 veh/h	20 km/h	55 km/h	800 veh/h
b	3 km	CD	500 veh/h	33 km/h	65 km/h	420 veh/h
c	4 km	AB	600 veh/h	50 km/h	55 km/h	270 veh/h

During the collapse scenario task, the volume of the closed path is detoured to the remaining ones according to the selected traffic assignment method. From the point of view of the infrastructure manager, it would be appropriate to minimize the overall system's disruption, while in a scenario without any supervisory intervention, the user optimum assignment offers a more realistic behaviour of drivers. In compliance with the data of Table 1 and to the network configuration of Figure 7, the results in terms of DII are presented in Table 2.

TABLE 2. DII results for the parameters of Table 1, network of Figure 7 and two traffic assignment methods.

Closed: Path "a". Detoured = 800 veh/h	Sys. Opt. Assignment		Usr. Equil. Assignment	
Alternative Paths:	b	c	b	c
Volume/capacity in post-hazard condit.	1.13	1.54	1.54	1.2
DII	1.1	4.0	2.4	2.3
Closed: Path "b". Detoured = 420 veh/h	Sys. Opt. Assignment		Usr. Equil. Assignment	
Alternative Paths:	a	c	a	c
Volume/capacity in post-hazard condit.	1.30	0.75	1.30	0.75
DII	2.6	1.3	2.6	1.3
Closed: Path "c". Detoured = 270 veh/h	Sys. Opt. Assignment		Usr. Equil. Assignment	
Alternative Paths:	a	b	a	b
Volume/capacity in post-hazard condit.	1.31	0.90	1.21	1.03
DII	3.8	1.1	2.6	1.6

From this simple example, it is evident that the system optimum assignment enhances the differences between alternatives, highlighting critical situations that might arise during a network disruption. On the contrary, this is not well understandable by local managers if the user equilibrium is

employed instead, as no greater differences are observed in terms of DIIs. Nevertheless, this example highlighted the flexibility of the proposed method, which can successfully accommodate various traffic assignment models. The framework, in this version, can handle a disruption at time, for each $p \in R^n_p$; multi-link failures might generate higher DIIs, whereas in such case, the probability of having multiple disruptions will be included in an updated version of the model. The Detour-Impact Index (DII) has been proposed here to summarize the influence that the closure of a certain path has on its users, by looking at the disruptions generated on other routes and compared to the initial conditions of the network, which might be already in a congested state, being not properly managed. The performance indicator is applied to a real-world scenario in the following section.

APPLICATION

The framework was tested in the municipalities of Massa and Carrara in Tuscany, Italy. This province suffered from high damages in the last decade, with two major disasters. One occurred in October 2011, where severe rainstorms caused the collapse of 11 bridges and damages up to 100 million euro (37), and another inundation in 2012 on the coastal area, with the collapse of several bridges and 24 million euro damages. In line with this scenario, and apart from major bridge collapses occurred in the last years (38), several failures on secondary road bridges revealed an unknown problem with a potential high impact (39), (40). A recent work developed by Puppio (41) has shown that 70% of the bridges is located on secondary infrastructures (with an average density of one bridge for each km) and among these, only 20% are found on official maps. Hence, it is not surprising if such collapses cause severe consequences for the population, leaving entire communities isolated. Thus, the proposed method has been applied to the Italian territory due to its vulnerability. The superimposition of road and hydraulic networks showed 756 crossings in the municipalities of Massa and Carrara, located in Northern Italy. The intersection with the O-D paths reduced the number of crossings to 123, as only the infrastructures on these routes are considered. Each settlement of these municipalities is connected to the civil protection headquarter, located in the city of Massa. The framework is here applied to three zones: (i) area of Avenza (Carrara), connected with suburban freeways to (ii) the city of Massa, (iii) mountain villages in Massa's municipality. The traffic composition, according to the average number of cars and trucks registered to the driving bureau, is 90% of cars and 10% of trucks in the municipality of Massa, 85% of cars and 15% of trucks in Carrara. In the following analyses, for each path the farthest village is assumed as Destination.

DII Computation

Between the first and the second zone, seven paths have been identified from the Civil Protection Headquarter of Massa to Avenza. The analysis showed that only five of them involve a possible bridge collapse as shown in **Figure 8**. The results in terms of DII are shown in **Figure 9**. When Path 1 is closed, path 4 is the most convenient alternative, with a saving of costs of 44% to path 5, 66% to path 2 and 100% compared to path 3. Conversely, when path 4 is closed, path 1 is the most economical alternative. Hence, path 1 and 4 can be considered strategic infrastructures, as the collapse of any infrastructure on other paths (2, 3, 5) can be dealt by means of these two routes. Furthermore, path 3 and 4 are those causing the overall major disruptions. Therefore, interventions could be planned to reduce the indirect costs on these two routes. Matrices as that displayed in **Figure 9** can be useful as support tool for specific improvements on the network, in order to reduce the higher impacts on detoured users. Thus, after a disruptive event, the connection between the cities of Massa and Avenza can be assured by several alternatives, with the DII's matrix as a practical tool for assessing the consequences on detoured users. A different situation is shown on the second case, where only one alternative path is available for each O-D pair. From the Civil Protection Headquarter to Massa's mountain area (zone 2 to zone 3) there are four destinations: Antona, Resceto, Casette and Forno. The last three have almost all routes in common, so that the collapse scenario is the same. All the other settlements in the area are located on the way to these three villages. For each destination, the analysis revealed only one alternative path as shown in **Figure 10**. The computation of the DII returns the following: $DII = 1.7$ when path A is closed and $DII = 2.6$ when path B is closed. In order to choose which is the most critical, a comparison between DIIs leads to the following statement: closing path B would cause costs 53% higher than closing path A. Even though this comparison seems to be unreasonable since the destinations are different, the alternative paths are mutually exclusives as visible in **Figure 10**. Thus,

since the costs are computed on each k-th link and, in this particular case, the diverted traffic volume is equal in both paths, B is more critical than A since path B corresponds to a greater DII.

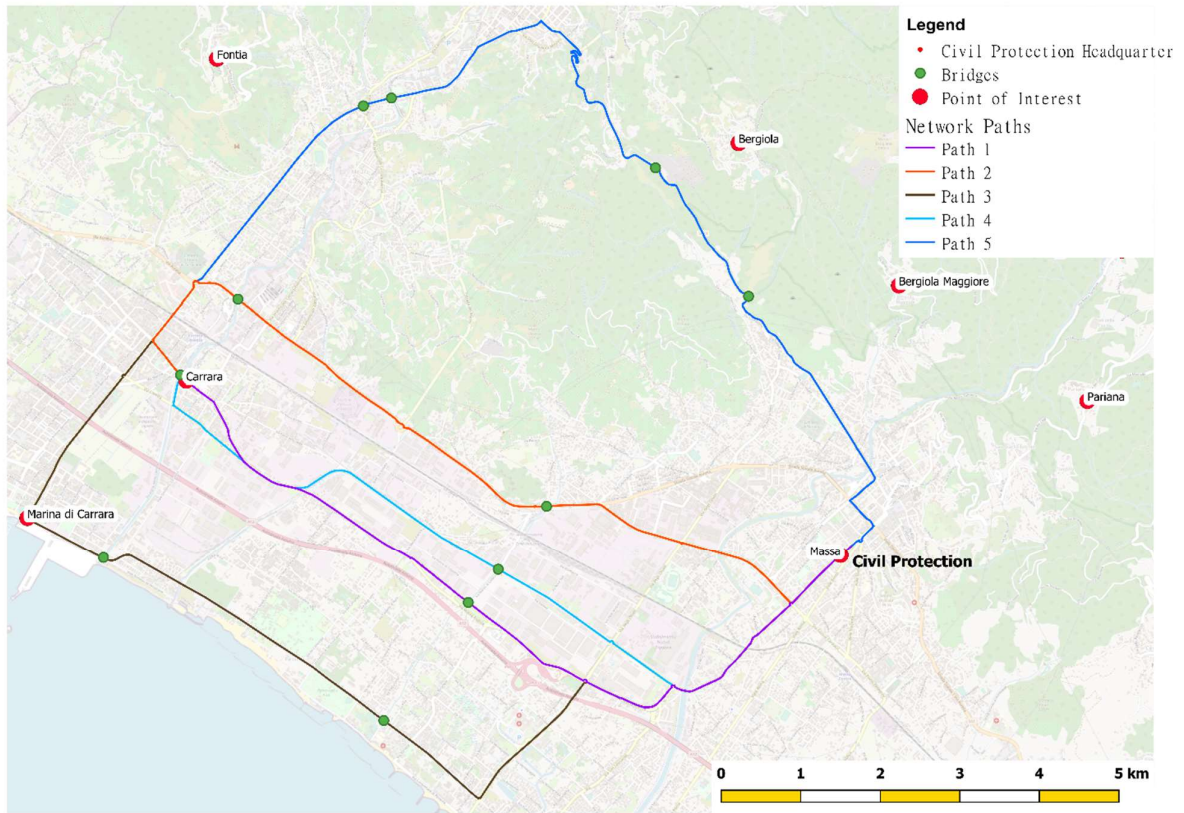


Figure 8. Paths from Civil Protection Headquarter to Avenza (Carrara)

DII		OPEN PATHS				
		Path 1	Path 2	Path 3	Path 4	Path 5
CLOSED PATHS	Path 1		5.3	6.4	3.2	4.6
	Path 2	2.5		6.3	3.1	4.1
	Path 3	1.7	3.3		1.9	2.8
	Path 4	3.2	6.3	7.4		5.2
	Path 5	2.1	4.2	5.3	2.5	

Figure 9. Detour-Impact Index for paths between zones 1 and 2

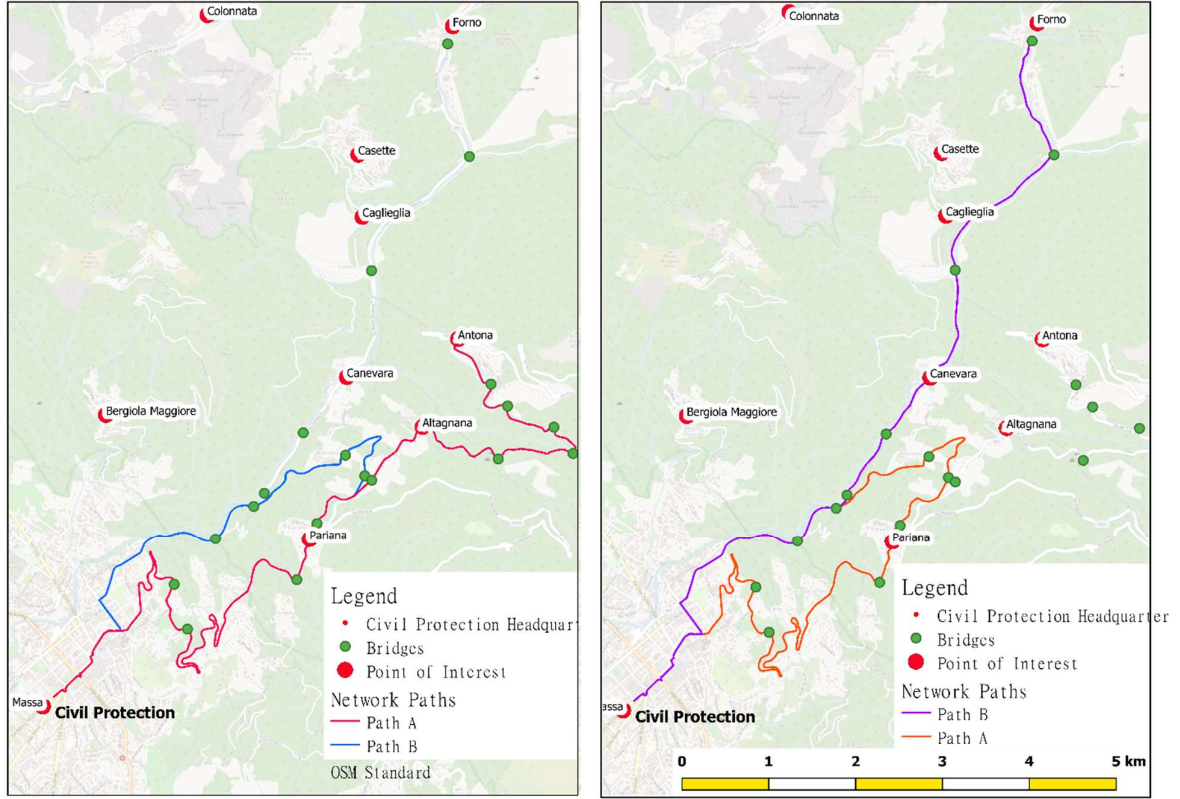


Figure 10. Paths from Civil Protection Headquarter to Antona (left), Forno (right)

Model validation

The validation of the model compares the travel time obtained from the proposed procedure in the no-hazard scenario to the travel time provided from Google Maps. The traffic analysis is computed using the same set of traffic data record. Statistical descriptive analysis of the sample returns that the error variability ranges from 0% to 40% for the lower bound interval, and from 0% to 33% for the upper bound. Dividing the sample between suburban and mountainous paths, the two measurements can be treated as independent. **Equation 7** was used to compare the error between the Estimated Time of Arrival (ETA) calculated using the proposed procedure (ETA_{method}) and the same quantity using web-based maps (ETA_{web}).

$$Error = |ETA_{method} - ETA_{web}| \quad (7)$$

TABLE 3. Errors between the ETAs of the proposed method and the web-based maps estimates.

		Statistics of errors	
		Suburban	Mountainous
Compared to Lower bound of Google Maps	Upper 95% confidence interval	39.4%	12.1%
	Mean error	32.1%	5.6%
	Lower 95% confidence interval	24.9%	0.9%
Compared to Upper bound of Google Maps	Upper 95% confidence interval	8.3%	32.0%
	Mean error	4.3%	27.2%
	Lower 95% confidence interval	0.3%	22.4%

The results in **Table 3** showed that the lowest errors (4.3% and 5.6%) appear in different boundaries of Google Maps ETA. This implies that the percentage of traffic explained by the model is considerably different between suburban and mountainous areas. The average ETA in suburban areas

is closer to the Google Maps ETA upper bound, while the opposite occurs for mountainous areas. This indicates that the indirect costs are underestimated on highlands compared to suburban ones. Taking these limitations into account, the results are satisfactory, with low errors (below 5.7%) in both areas.

CONCLUSIONS

Lessons learnt from past events highlight the key role of the road network usability after a bridge collapse. This aspect is particularly important for countryside and suburban areas, where the disruption of just one apparently secondary infrastructure might cause the isolation of entire communities. Moreover, the availability of data on rural areas can limit existing approaches. This is particularly relevant for traffic data. Furthermore, road performance indicators rely on generalised users' costs functions, while the combination of trip's purpose, traffic composition and vehicles' operative costs should be explicitly accounted for. This paper addressed these issues proposing a new aggregate metric, known as Detour-Impact Index (DII). The performance indicator combines traditional impact metrics with innovative algorithm to address challenges on rural contexts. Indeed, traffic data availability has been solved using a new web-based method, able to transform qualitative information into quantitative volumes of vehicles. Furthermore, the method introduced a delay-cost function (DC) and a vehicle's operational cost (VOC). This allowed to explicitly account for the driver's time cost function, the trip's purpose and the traffic composition. The method is the first attempt to combine data availability issues, roads' disruptions and include the evaluation of users' specific consequences. As such, the method is limited by several assumptions, which are critically addressed. These include the mean LOS velocity as the traffic speed during the conversion from qualitative to quantitative data. Despite this high-handed decision, the experimental results were found in good agreement with the predicted values. The validation of the model was verified by a statistical analysis where the error was 4.3% for suburban roads and 5.6% for mountainous ones. Thus, there is evidence to suggest that assuming the mean speed for each LOS as the mean speed of vehicle's flow, is an acceptable decision. It can also be inferred that the street class is a critical parameter to the mean speed assumption. Indeed, each street category has distinctive values of speed range, and these are summarized in specific tables in the HCM. Thus, since these are based on semi-empirical studies, it is reasonable to think that the distribution of speed values on streets follows a normal distribution. Thus, the mean value is also the most frequent one. This can explain why the method works in good agreement with real-case scenarios. This procedure is not substitutive of the more reliable traffic counters, but it allows to produce a first quantitative estimate of the traffic on roads where no traffic data is available. Each path is classified as being more or less critical to the network, based on a single-link failure. This feature may lead to the underestimation of DIIs, since a multi-link disruption would lead to higher values. Although this issue is not for granted, in this situation a different method (i.e. a probabilistic approach) should be assumed when several disruptions occur at time. This is because in a multi-link failure the worst-case scenario should be reasonably supported by a probability of occurrence. Future challenges are being made incorporating a capacity-reduction likelihood. A further expansion might include a refined traffic volumes calculation applying the same method on other datasets. The proposed framework, in this first version, might be a useful tool to prevent situations in which the detour implies a significant increase of users' costs. The lack of network redundancy on rural areas and critical scenarios can be also highlighted.

ACKNOWLEDGMENTS

The first, third and sixth authors acknowledge that, this work was partly financed by FEDER funds through the Competitivity Factors Operational Programme - COMPETE and by national funds through FCT Foundation for Science and Technology within the scope of the project POCI-01-0145-FEDER-007633. This work was supported by the FCT Foundation for Science and Technology under Grant SFRH/BD/145478/2019.

AUTHOR CONTRIBUTIONS

The authors confirm contribution to the paper as follows: study conception and design: A. Pucci, H. S. Sousa, J. C. Matos; data collection: A. Pucci; analysis and interpretation of results: A. Pucci, H. S. Sousa, L. Giresini; draft manuscript preparation: A. Pucci, M. L. Puppio, M. Sassu. All authors reviewed the results and approved the final version of the manuscript.

REFERENCES

1. Wisetjindawat W, Derrible S, Kermanshah A. Modeling the Effectiveness of Infrastructure and Travel Demand Management Measures to Improve Traffic Congestion during Typhoons. *Transportation Research Record*. 2018 Aug 27;2672(1):43–53. Available from: <https://doi.org/10.1177/0361198118791909>
2. Capacci L, Biondini F, Titi A. Lifetime seismic resilience of aging bridges and road networks. *Structure and Infrastructure Engineering*. 2020;16(2):266–86. Available from: <https://doi.org/10.1080/15732479.2019.1653937>
3. Porta S, Crucitti P, Latora V. The network analysis of urban streets:a primal approach. *Envir. and Plann. B: Plann. and Design*. 2006;33:705-725. <https://doi.org/10.1068/b32045>
4. Inkoom S, Sobanjo JO. Reliability Importance as a Measure of Bridge Element Condition Index for Deteriorating Bridges. *Transportation Research Record*. 2019 Jul 11;2673(12):327–38. Available from: <https://doi.org/10.1177/0361198119862627>
5. Mattsson L, Jenelius E. Vulnerability and resilience of transport systems – A discussion of recent research. *Transportation Research Part A*. 2015;81:16–34.
6. Jiang Y, Wang Y, Szeto WY, Chow AHF, Nagurney A. Probabilistic assessment of transport network vulnerability with equilibrium flows. *International Journal of Sustainable Transportation*. 2020;1–12. Available from: <https://doi.org/10.1080/15568318.2020.1770904>
7. Scott DM, Novak DC, Aultman-Hall L, Guo F. Network Robustness Index : A new method for identifying critical links and evaluating the performance of transportation networks. *Journal of Transport Geography*. 2006;14:215–27.
8. Nagurney A, Qiang Q. A network efficiency measure for congested networks. *Europysics Letters*. 2007;79(3):38005.
9. Sullivan JL, Novak DC, Aultman-Hall L, Scott DM. Identifying critical road segments and measuring system-wide robustness in transportation networks with isolating links : A link-based capacity-reduction approach. *Transportation Research Part A*. 2010;44(5):323–36. Available from: <http://dx.doi.org/10.1016/j.tra.2010.02.003>
10. Rupi F, Bernardi S, Rossi G. The Evaluation of Road Network Vulnerability in Mountainous Areas : A Case Study. *New Spatial Economy*. 2015;15:397–411.
11. Xu X (Alex), Fakhroosavi F, Zockaie A, Mahmassani HS. Estimating Path Travel Costs for Heterogeneous Users on Large-Scale Networks: Heuristic Approach to Integrated Activity-Based Model–Dynamic Traffic Assignment Models. *Transportation Research Record*. 2017 Jan 1;2667(1):119–30. Available from: <https://doi.org/10.3141/2667-12>
12. Bagloee AS, Sarvi M, Wolshon B, Dixit V. Identifying critical disruption scenarios and a global robustness index tailored to real life road networks. *Transportation Research Part E*. 2017;98:60–81. Available from: <http://dx.doi.org/10.1016/j.tre.2016.12.003>
13. Kermanshah A, Derrible S. Robustness of road systems to extreme flooding: using elements of GIS, travel demand, and network science. *Natural Hazards*. 2017;86(1):151–64.
14. Arrighi C, Pregolato M, Dawson RJ, Castelli F. Preparedness against mobility disruption by floods. *Science of the Total Environment*. 2019;654:1010–22. Available from: <https://doi.org/10.1016/j.scitotenv.2018.11.191>

15. Khan SM, Islam S, Khan MDZ, Dey K, Chowdhury M, Huynh N, et al. Development of Statewide Annual Average Daily Traffic Estimation Model from Short-Term Counts: A Comparative Study for South Carolina. *Transportation Research Record*. 2018 Nov 8;2672(43):55–64. Available from: <https://doi.org/10.1177/0361198118798979>
16. Zhang X, Chen M. Enhancing Statewide Annual Average Daily Traffic Estimation with Ubiquitous Probe Vehicle Data. *Transportation Research Record*. 2020 Jun 21;2674(9):649–60. Available from: <https://doi.org/10.1177/0361198120931100>
17. Selby B, Kockelman KM. Spatial prediction of traffic levels in unmeasured locations : applications of universal kriging and geographically weighted regression. *Journal of Transport Geography*. 2013;29:24–32. Available from: <http://dx.doi.org/10.1016/j.jtrangeo.2012.12.009>
18. Alsobky A, Mousa R. Estimating free flow speed using Google Maps API: accuracy, limitations, and applications. *Advances in Transportation Studies, an International Journal*. 2020;50:49–64.
19. Nair DJ, Gilles F, Chand S, Saxena N, Dixit V. Characterizing multicity urban traffic conditions using crowdsourced data. *PLoS ONE*. 2019;14(3):1–16.
20. Petrovska N, Stevanovic A. Traffic Congestion Analysis Visualisation Tool. In: 2015 IEEE 18th International Conference on Intelligent Transportation Systems. Las Palmas de Gran Canaria: IEEE; 2015. p. 1489–94.
21. Sarvepalli A, Davis B. Multiple Uses of Big Data for Model Validation and Express Lanes Traffic Forecasts. *Transportation Research Record*. 2020 Aug 20;2674(11):87–100. Available from: <https://doi.org/10.1177/0361198120942222>
22. Pulugurtha S., Penmetsa P, Duddu VR. Travel time, reliability, additional trip time, willingness to pay and their values by socio-economic factors. *Advances in Transportation Studies, an International Journal*. 2019;49:31–46.
23. Zhang N, Alipour A. Two-Stage Model for Optimized Mitigation and Recovery of Bridge Network with Final Goal of Resilience. *Transportation Research Record*. 2020 Jul 22;2674(10):114–23. Available from: <https://doi.org/10.1177/0361198120935450>
24. Togia H, Francis OP, Kim K, Zhang G. Segment-Based Approach for Assessing Hazard Risk of Coastal Highways in Hawai'i. *Transportation Research Record*. 2019 Jan 1;2673(1):83–91. Available from: <https://doi.org/10.1177/0361198118821679>
25. Giresini L, Puppio ML, Sassu M. Collapse of corrugated metal culvert in Northern Sardinia: analysis and numerical simulations. *Special Issue of International Journal of Forensic Engineering*. 2016;3(1–2):69–85.
26. Kalendher Lebbe MF, Lokuge W, Setunge S, Zhang K. Failure mechanisms of bridge infrastructure in an extreme flood event. In: *Proceedings of the First International Conference on Infrastructure Failures and Consequences*. Melbourne: Emerald Group Publishing Limited; 2014. p. 124–32.
27. Gervásio H, Simões L da S. Life-cycle social analysis of motorway bridges. *Structure and Infrastructure Engineering*. 2013;9(10):1019–39.
28. Jedlička K, Hájek P, Čada V, Martolos J, Šťastný J, Beran D, et al. Open Transport Map - Routable OpenStreetMap. In: Paul Cunningham and Miriam Cunningham, editor. *IST-Africa 2016 Conference Proceedings*. Durban: IIMC International Information Management

- Corporation; 2016. p. 1–11.
29. Commissione Tecnica per la Microzonazione Sismica. Condizione limite per l'emergenza (CLE). Rome; 2014.
 30. Schneck A, Nokel K. Accelerating Traffic Assignment with Customizable Contraction Hierarchies. *Transportation Research Record*. 2020;2674(1):188–96.
 31. Pella H, Ose K. Network Analysis and Routing with QGIS. In: Baghdadi N, Mallet C, Zribi M, editors. *QGIS and Applications in Water and Risks*. First. London: ISTE Ltd and John Wiley & Sons, Inc.; 2018. p. 105–44.
 32. National Institutes of Health. ImageJ [Internet]. 1997 [cited 2020 Nov 10]. Available from: <https://imagej.nih.gov/ij/>
 33. Transportation Research Board. *Highway Capacity Manual*. Washington D.C.; 2010.
 34. Google LLC. Google Maps Platform FAQs [Internet]. 2020 [cited 2020 Nov 10]. Available from: <https://developers.google.com/maps/faq>
 35. Gusev M. GNM plugin for QGIS [Internet]. 2015 [cited 2020 Nov 11]. Available from: https://github.com/nextgis/gnm_qgis
 36. Sassu M, Giresini L, Puppio ML. Failure scenarios of small bridges in case of extreme rainstorms. *Sustainable and Resilient Infrastructure*. 2017;2(3):108–16. Available from: <http://dx.doi.org/10.1080/23789689.2017.1301696>
 37. Bini C, Ciampi P, Cressanti S, Fattorini R, Fortini W, Lucchi C, et al. Cosa insegna il fiume [Internet]. Regione Toscana, editor. Florence: Toscana Notizie; 2012. 201 p. Available from: www.toscana-notizie.it
 38. Bazzucchi F, Restuccia L, Ferro GA. Considerations over the Italian road bridge infrastructure safety after the Polcevera viaduct collapse: past errors and future perspectives. *Frattura ed Integrità Strutturale*. 2018;12(46):400–21.
 39. Stochino F, Fadda ML, Mistretta F. Low cost condition assessment method for existing RC bridges. *Engineering Failure Analysis*. 2018;86(December 2017):56–71. Available from: <https://doi.org/10.1016/j.engfailanal.2017.12.021>
 40. Stochino F, Fadda ML, Mistretta F. Assessment of RC Bridges integrity by means of low-cost investigations. *Design of Civil Environmental Engineering*. 2018;46(October):216–25.
 41. Puppio ML. Safety Assessment and Strengthening of Short Span Bridges in case of Extreme Rainstorms. PhD Thesis. University of Pisa; 2018.